Supporting Information

Effect of metal oxidation state on FRET: A Cu(I) silent but selectively Cu(II) responsive fluorescent reporter and its bioimaging applications

Siddhartha Pal,[a] Buddhadeb Sen,[a] Somenath Lohar,[a] Manjira Mukherjee,[a] Samya Banerjee,[b] and Pabitra Chattopadhyay[a]*

[a]*Department of Chemistry, Burdwan University, Golapbag, Burdwan, 713104, India,*

[b]*Department of Inorganic and Physical Chemistry, Indian Institute of Science, Bangalore, 560012, India*

Corresponding author: pabitracc@yahoo.com

Contents

Materials and physical measurements

The analytical grade solvents and the other reagent grade chemicals consumed in this work were purchased from commercial sources and used as received. Perkin Elmer 2400 CHN elemental analyzer was utilized for elemental analyses (C, H and N). A UV-1800 and a Prestige-21 spectrophotometers made by Shimadzu, Japan were used for recording electronic spectra and IR spectra, respectively. A Shimadzu (model UV-1800) spectrophotometer was used for recording UV-vis spectra. IR spectra were recorded using Prestige-21 SHIMADZU FTIR spectrometer. ^{1}HNMR spectra were collected from a JEOL 400 spectrometer using $CDCl_3$ solution. Electrospray ionization (ESI) mass spectra were recorded on a Qtof Micro YA263 mass spectrometer. All pH solutions were done by a Systronics digital pH meter (model 335) using either 50 mM HCl or NaOH solution. A vibrating sample magnetometer PAR 155 model was used to measure the room temperature magnetic susceptibility. Steady-state fluorescence emission and excitation spectra were recorded with a Hitachi-7000 spectrofluorimeter. Time-resolved fluorescence lifetime measurements were performed using a HORIBA JOBIN Yvon picosecond pulsed diode laser-based time-correlated single-photon counting (TCSPC) spectrometer from IBH (UK) at λ_{ex}= 340 nm and MCP-PMT as a detector. Emission from the sample was collected at a right angle to the direction of the excitation beam maintaining magic angle polarization (54.71). Maintaining the resolution of 28.6 ps per channel, the full width at half-

maximum (FWHM) of the instrument response function was 250 ps. IBH DAS 6.2 data analysis software was used to fit the data to multiexponential functions after deconvolution of the instrument response function by an iterative reconvolution technique and here, reduced w2 and weighted residuals served as parameters for goodness of fit. Redox potentials were recorded in CHI620D potentiometer in dry acetonitrile using TBAP as supporting electrolyte at room temperature. The experimental solutions were deoxygenated by bubbling with research grade dinitrogen. The reported potentials are uncorrected for junction potential and are expressed with reference to Ag/AgCl electrode.

The luminescence property of **HL** was checked in HEPES buffer (1 mM, pH 7.4; acetonitrile/water: 1/5, v/v) at 25 °C. The study of effect of pH was carried out in 100 mM HEPES buffer solution by adjusting the pH using HCl or NaOH. *In vivo* study was performed at biological pH ~7.4 with 100 mM HEPES buffer solution. The stock solutions (~ 10^{-2} M) for the selectivity study of **HL** towards different metal ions were prepared taking nitrate salts of sodium, potassium, aluminium(III), chromium(III), silver(I); acetate salt of manganese(II), zinc(II); chloride salts of nickel(II), cobalt(II), mercury(II), calcium(II), magnesium(II), iron(III); iron(II) sulphate in HEPES buffer (1 mM, pH 7.4; acetonitrile/water: 1/5, v/v) solvent. In this selectivity study the amount of these metal ions was a hundred times greater than that of the probe (**HL**) used. Fluorimetric titration was performed with cupric nitrate and $[Cu(AN)_4]ClO_4$ in HEPES buffer (1 mM, pH 7.4; acetonitrile/water: 1/5, v/v) solvent varying the metal concentration 0 to 20 μM and the probe concentration was 10 μM.

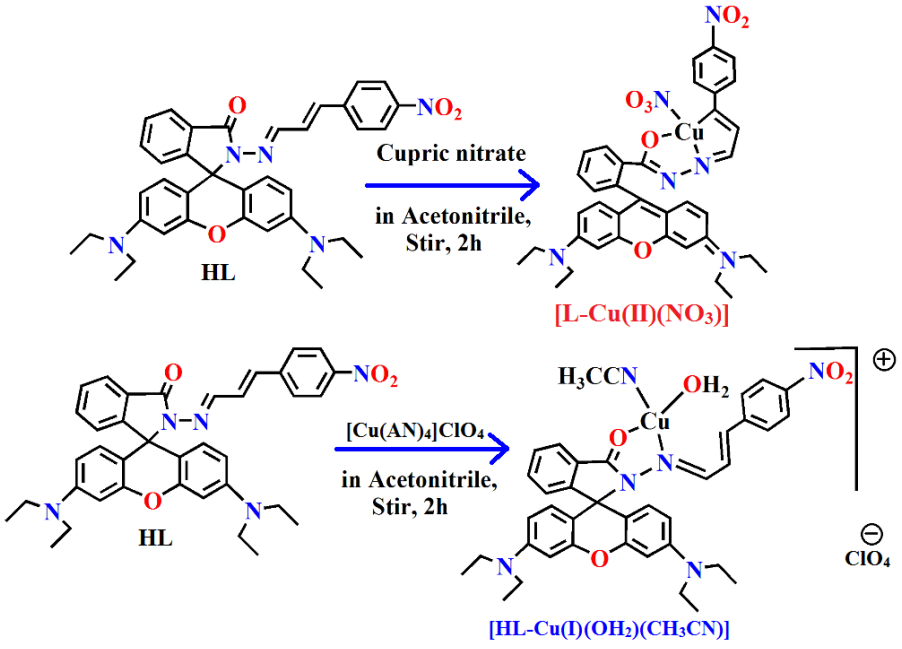

Scheme S1 Schematic representation of synthesis of the complexes

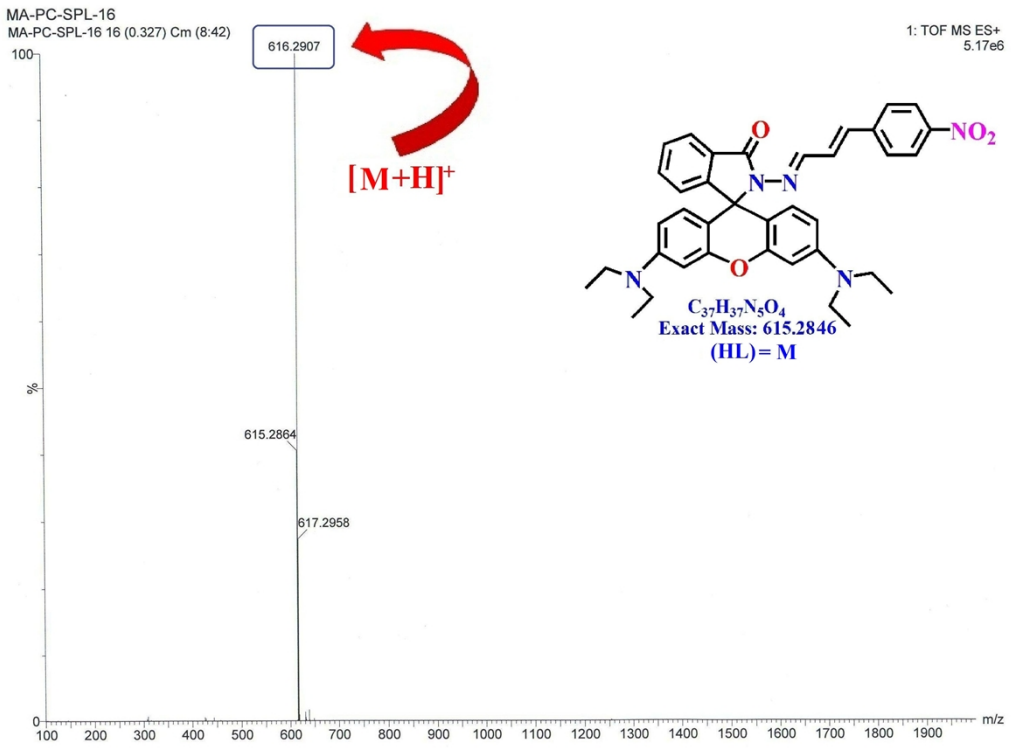

Fig. S1 ESI-MS of the probe (**HL**) in acetonitrile

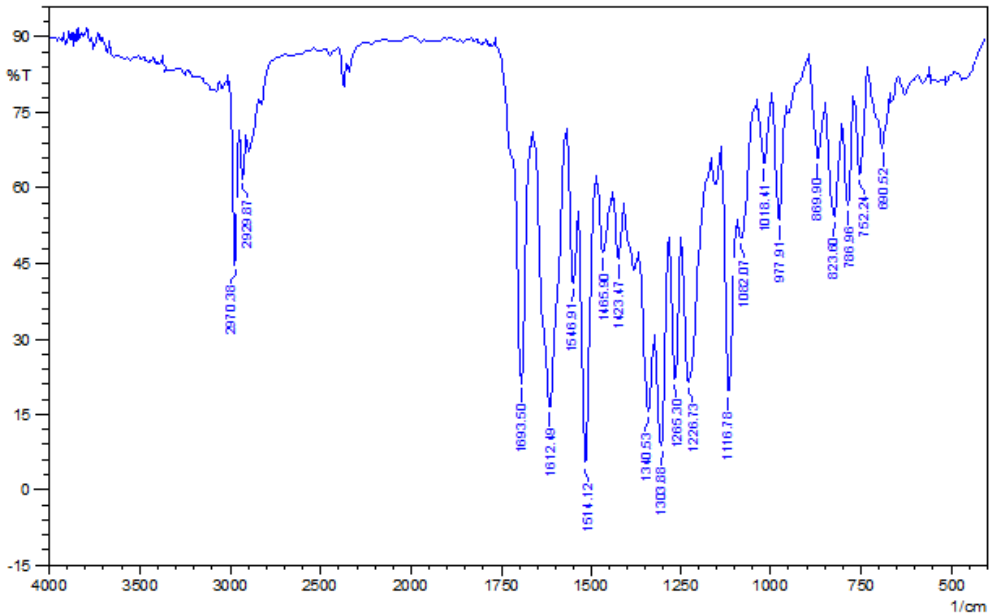

Fig. S2 FTIR spectrum of **HL**

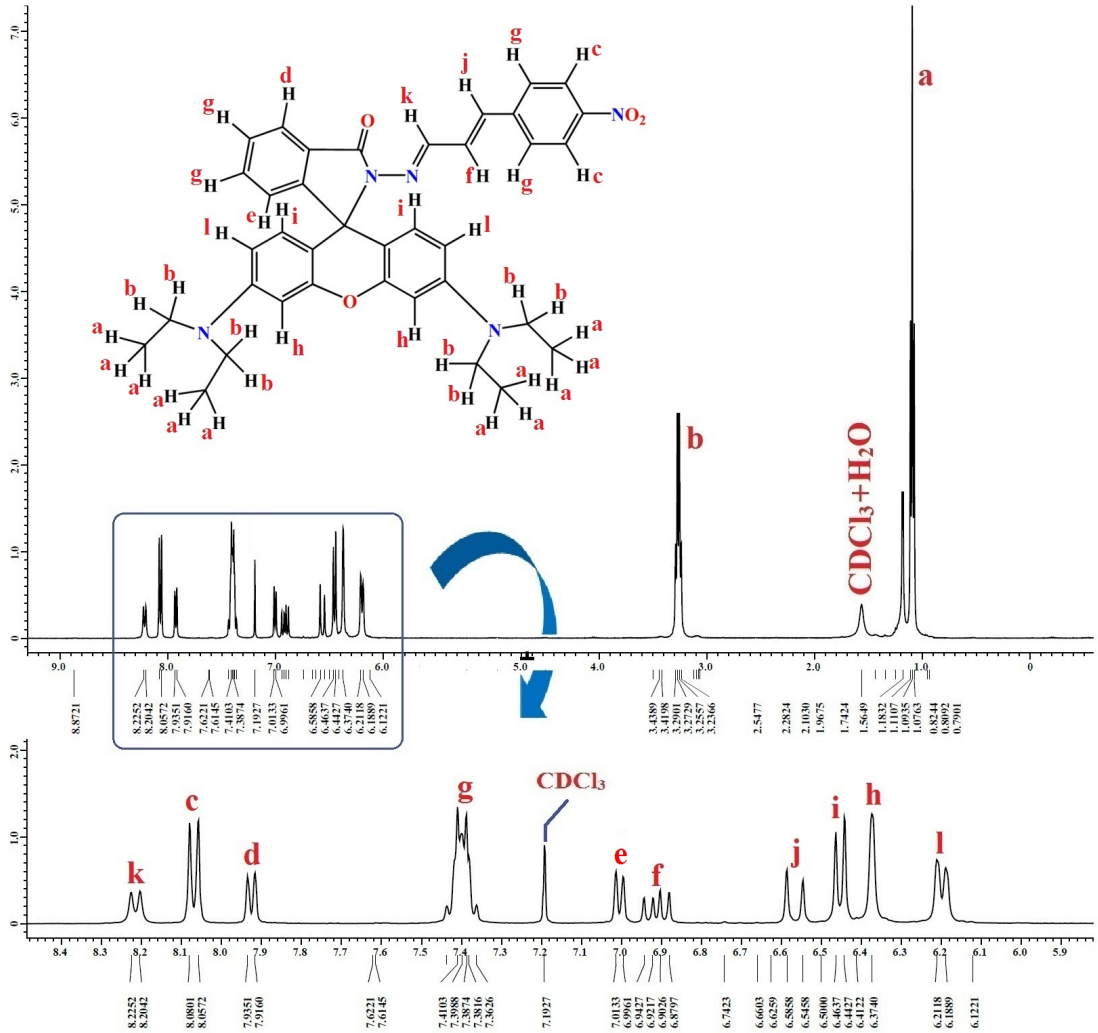

Fig. S3 ^{1}H NMR of the probe (**HL**) in $CDCl_3$

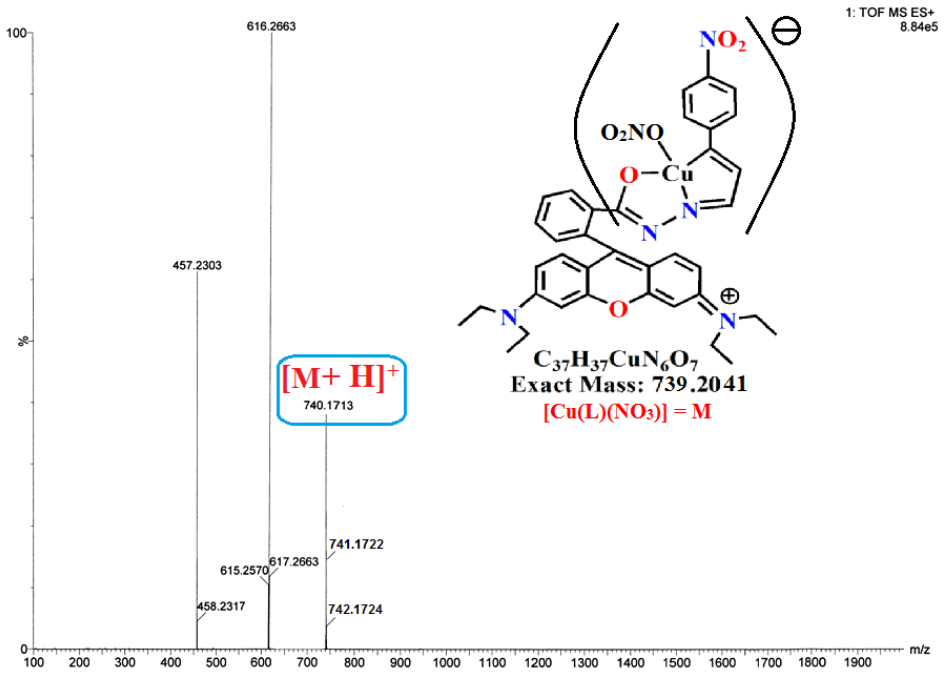

Fig. S4 ESI-MS of **Cu(II)** complex by $Cu(NO_3)_2$ salt in acetonitrile

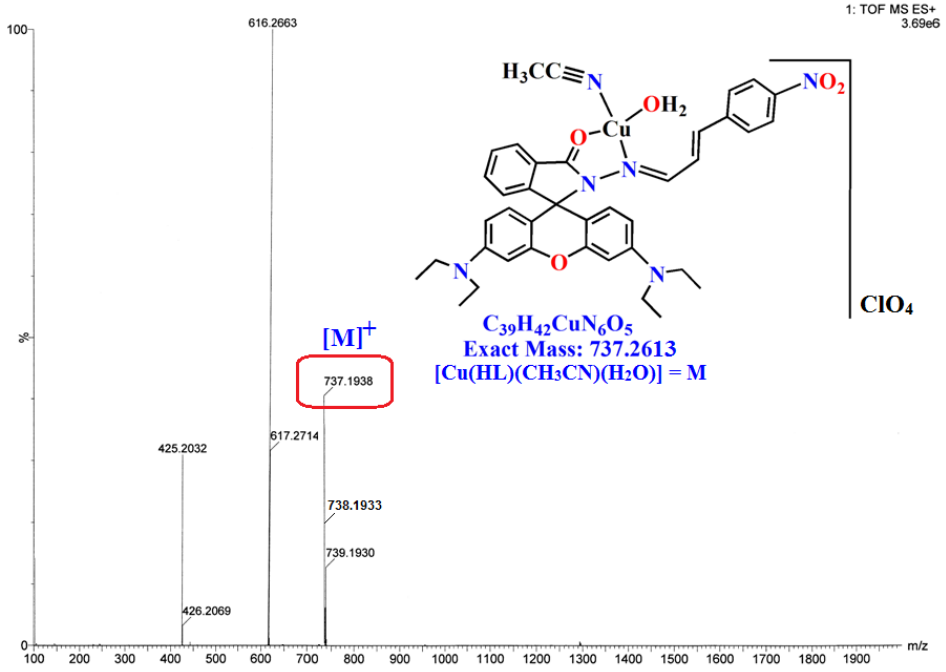

Fig. S5 ESI-MS of **Cu(I)** complex by $[Cu(AN)_4ClO_4]$ salt in acetonitrile

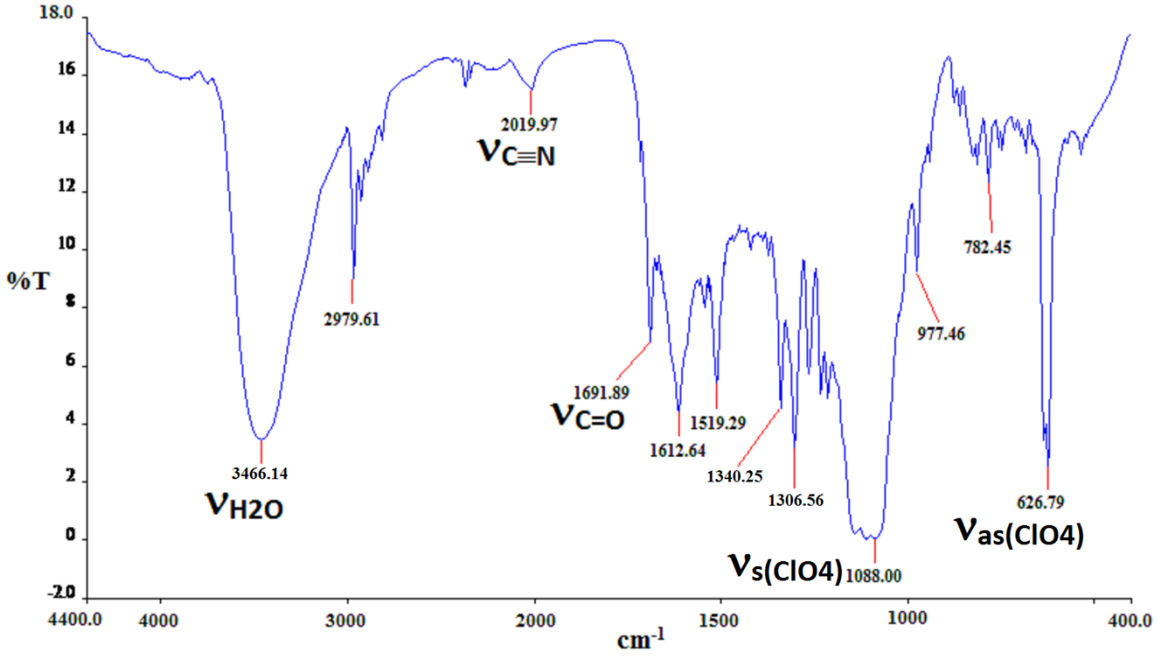

Fig. S6 FTIR spectrum of **[Cu^{I}(HL)(H_2O)(CH_3CN)]ClO_4**

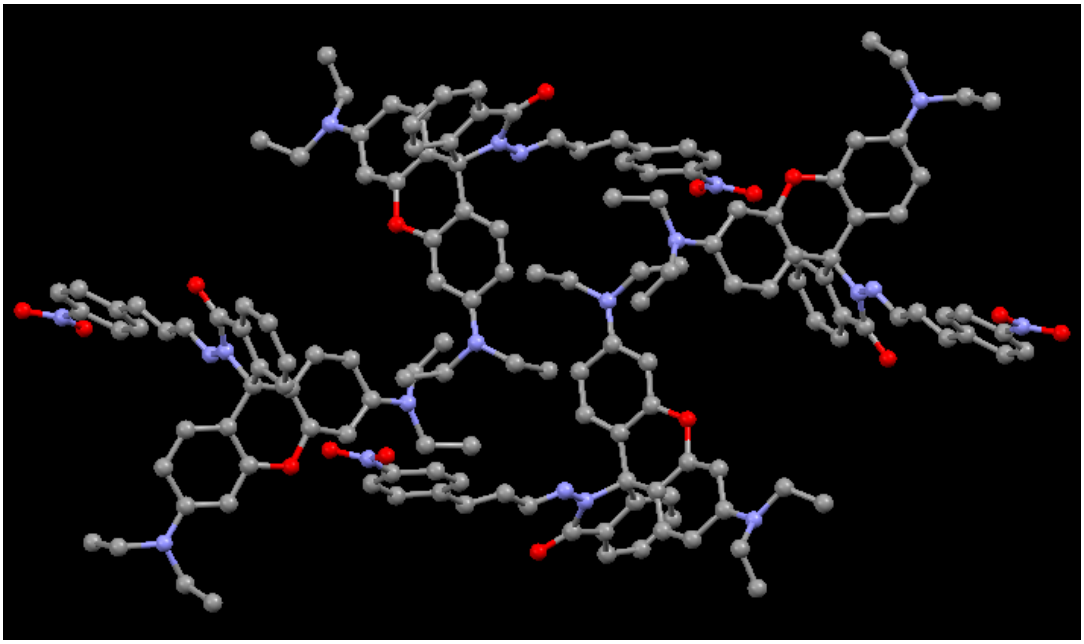

Fig. S7 Crystal packing arrangement of **HL**

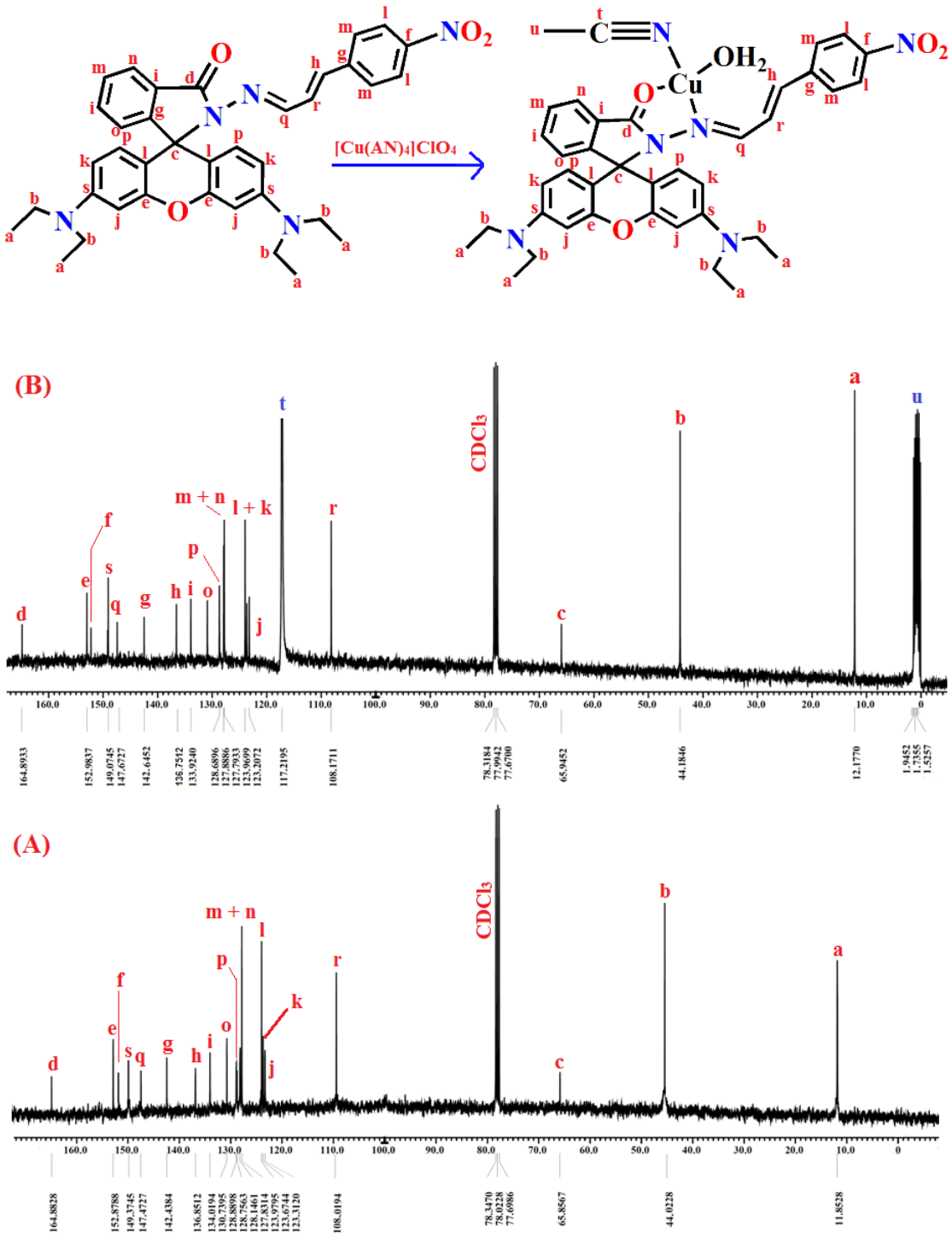

Fig. S8 Partial ^{13}C NMR spectra for (A) **HL** and (B) **Cu(I)** complex in $CDCl_3$

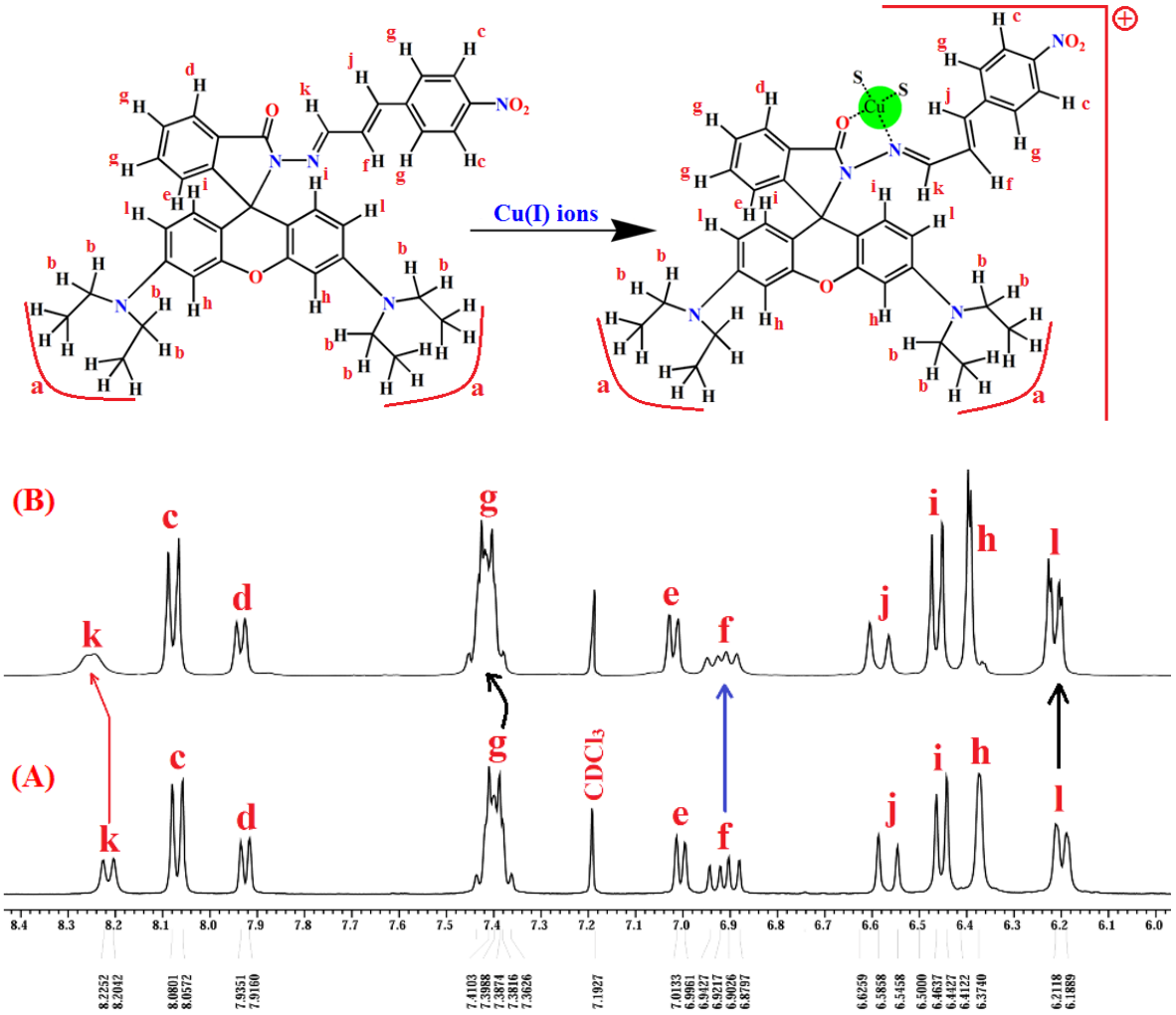

Fig. S9 Partial ^{1}H NMR titration with Cu(I) ions. [(A) **HL** and (B) **HL : Cu(I)** (1:1)]

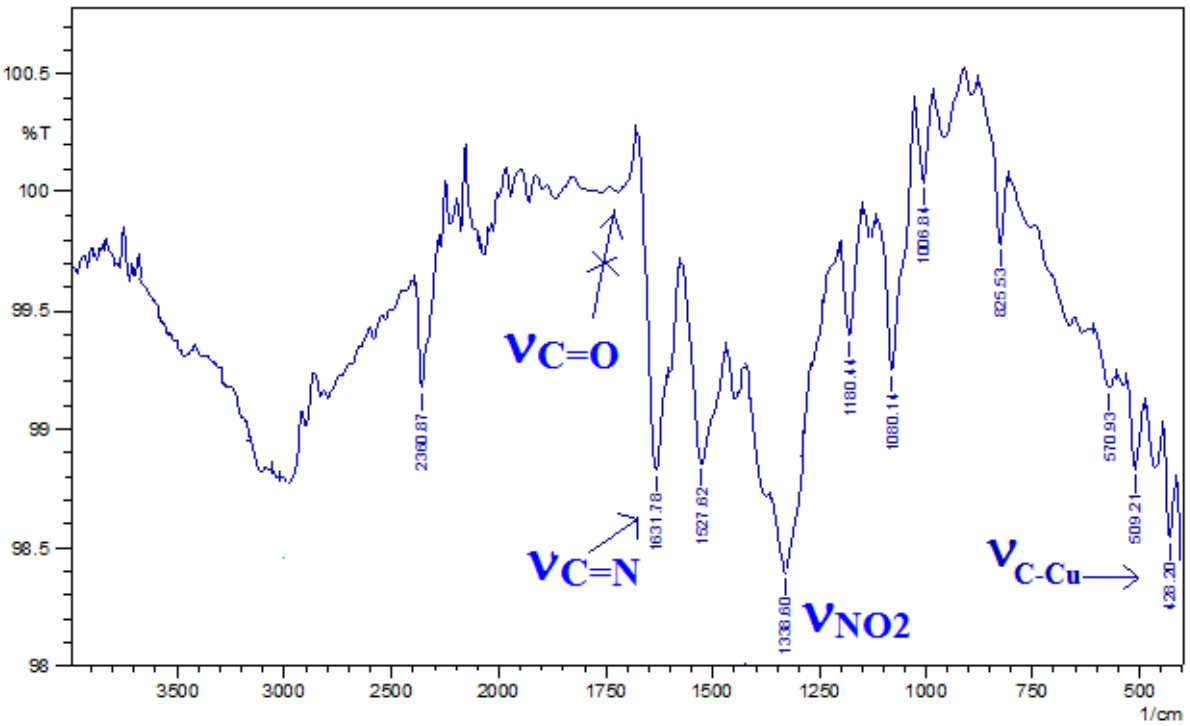

Fig. S10(a) FTIR spectrum of **[[Cu^{II}(L)(Cl)] (3)**

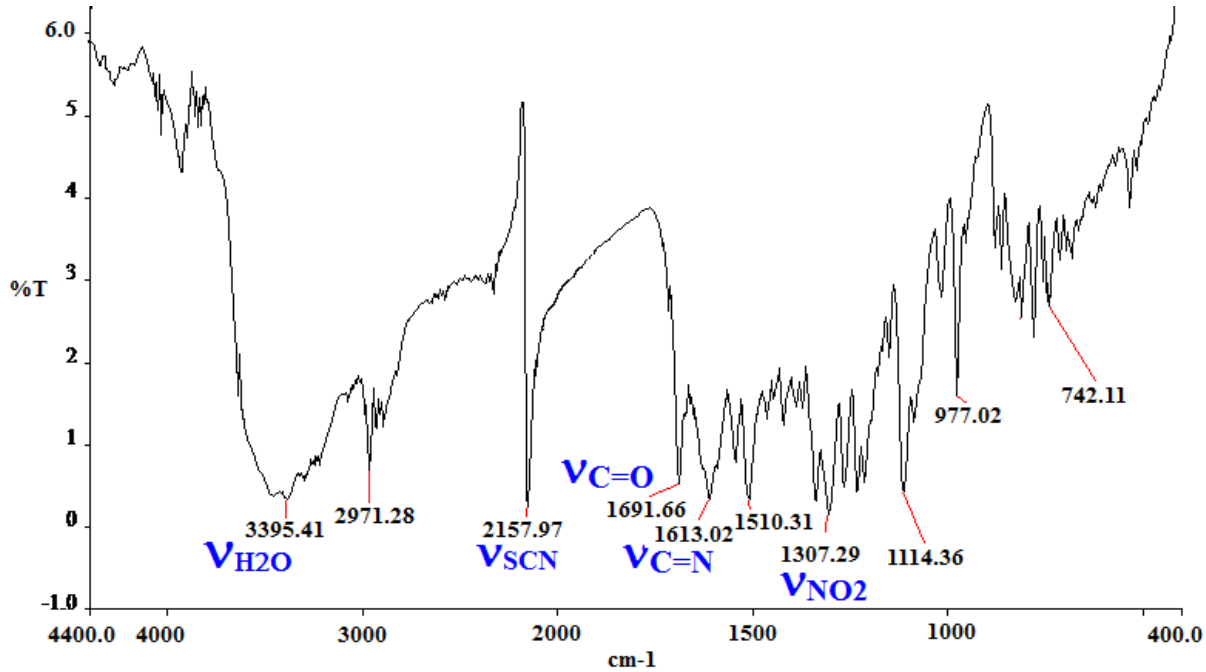

Fig. S10(b) FTIR spectrum of **[Cu^{I}(HL)(H$_2$O)(CH$_3$CN)]SCN**

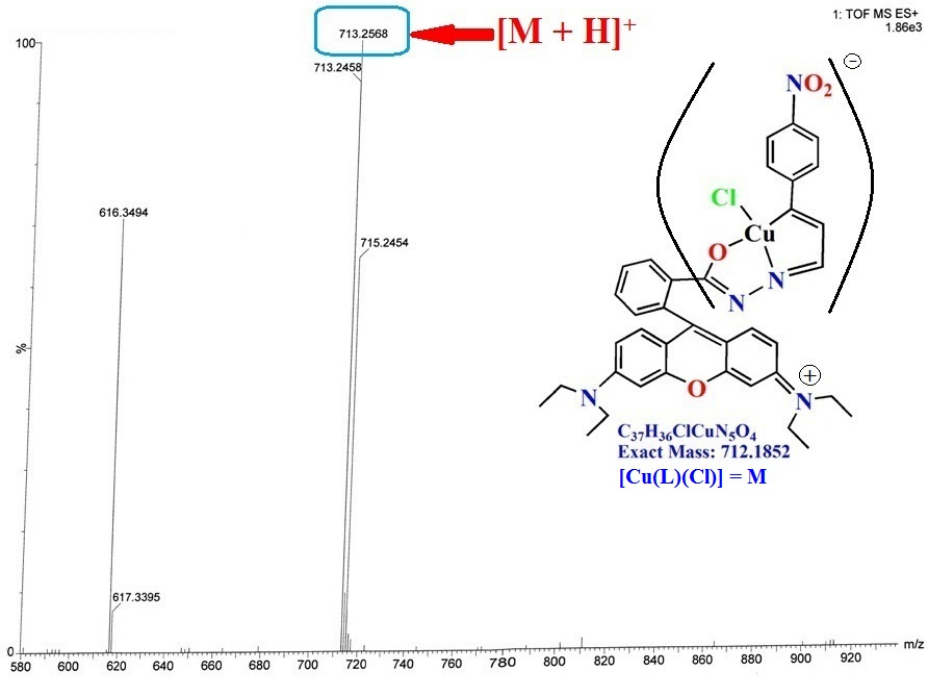

Fig. S11 ESI-MS of **Cu(II)** complex **(3)** by $CuCl_2$ salt in acetonitrile

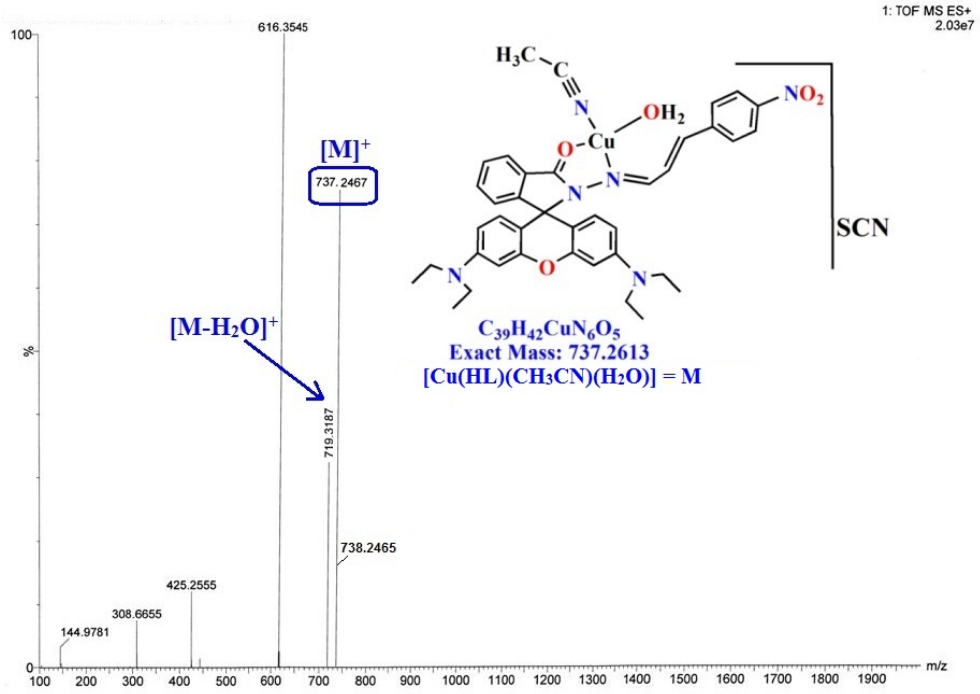

Fig. S12 ESI-MS of **Cu(I)** complex (**4**) by CuSCN salt in acetonitrile

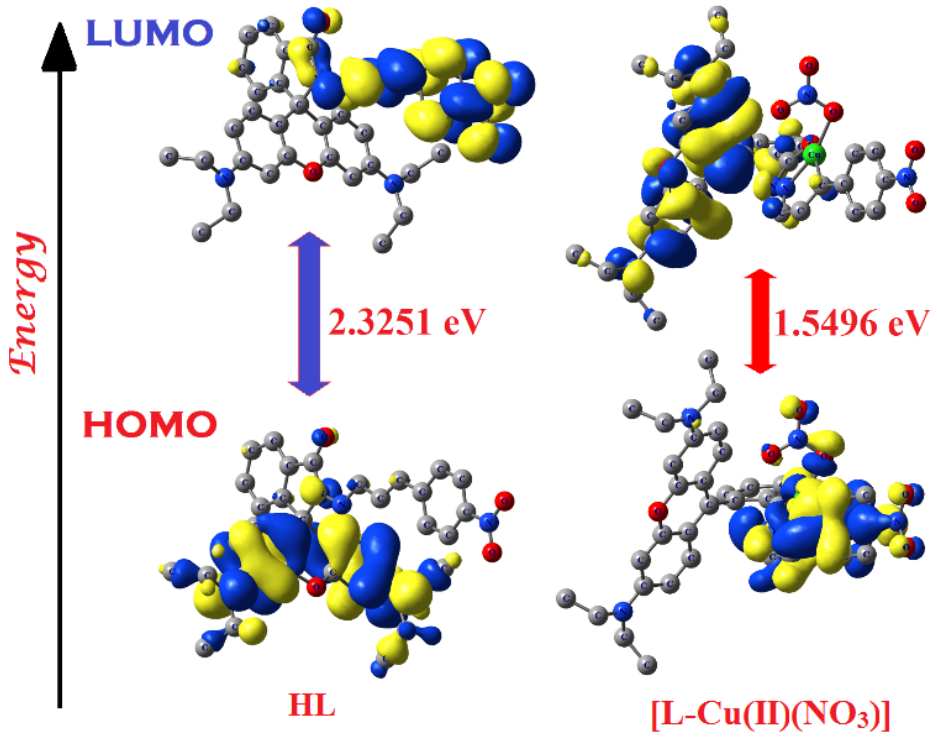

Fig. S13 π-MO's distribution and energy gap between HOMO and LUMO of **HL** and **[Cu(L)(NO$_3$)]** complex

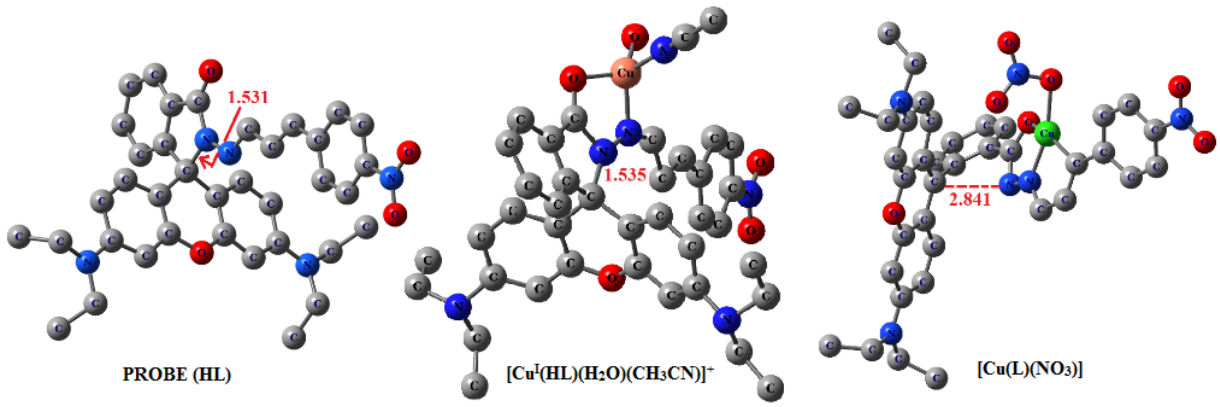

Fig. S14 Geometries optimization and important bond distances (Å) of rhodamine derivative **HL** and its complexes with Cu(I) and Cu(II). Hydrogens are omitted for clarity

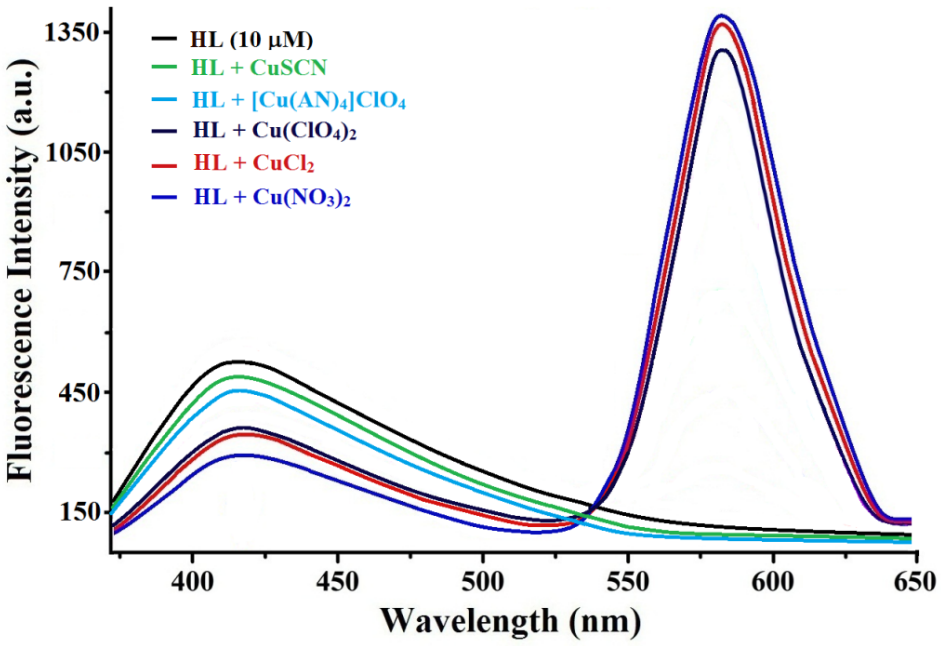

Fig. S15 Fluorescence spectra of **HL** with different Cu-salt in 1:1 ratio

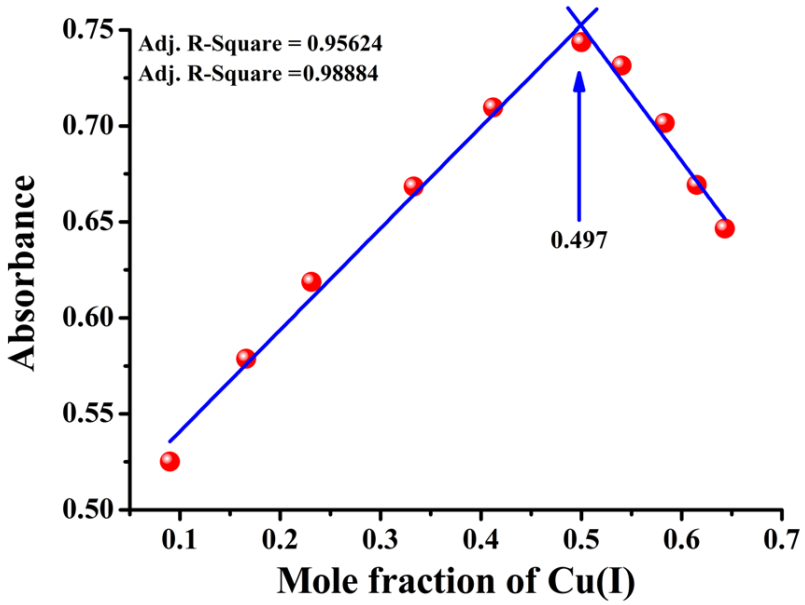

Fig. S16 Job's plot analysis of **HL : Cu(I)** ions from UV-Vis titration showing 1:1 stoichiometry

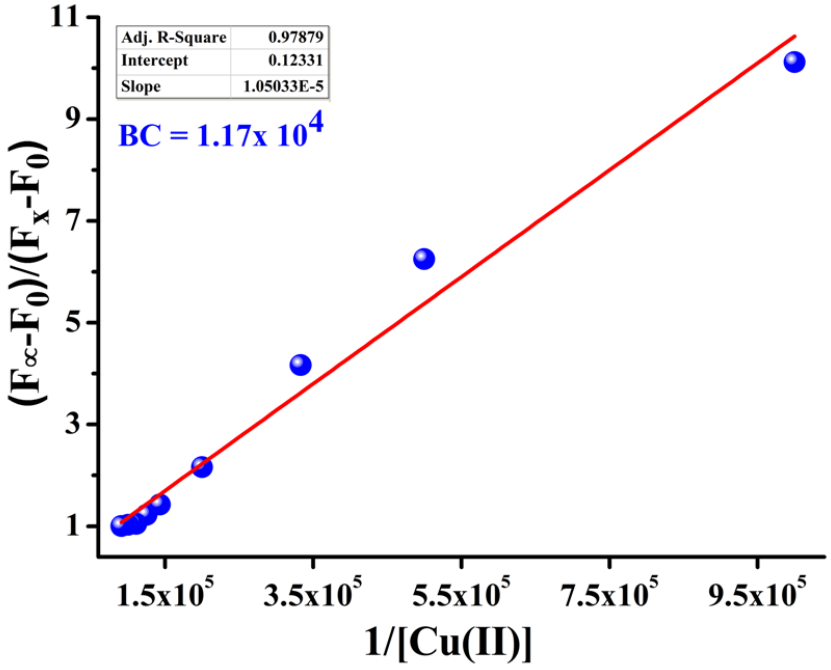

Fig. S17 Binding constant (K) value 1.17 X 10^4 M^{-1} determined from the interactions of **HL** with Cu(II) ions in HEPES buffer (1 mM, pH 7.4; acetonitrile/water: 1/5, v/v) at 25 °C

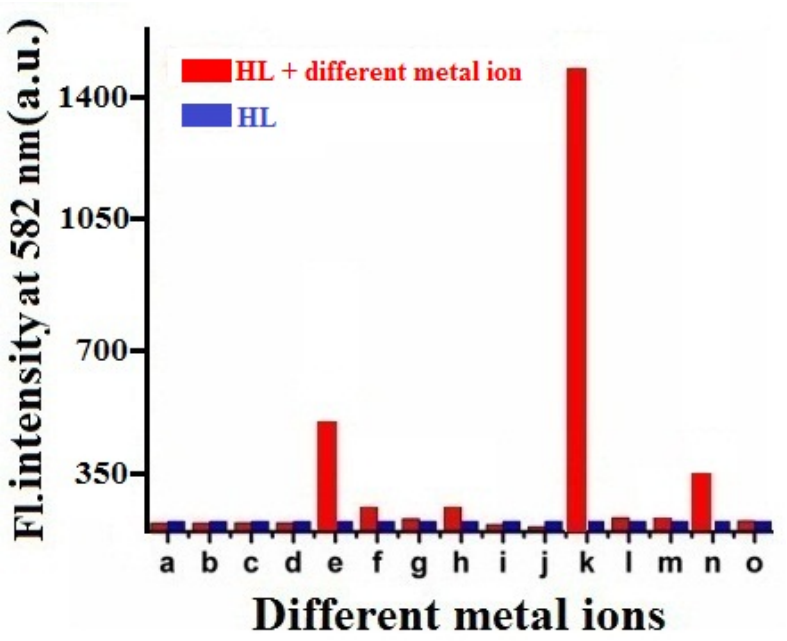

Fig. S18 Fluorescence intensity assay of **HL** in presence of different metal ions in HEPES buffer (1 mM, pH 7.4; acetonitrile/water: 1/5, v/v) at 25 °C (λ_{ex} = 365 nm), (a) Na^+, (b) K^+, (c) Ca^{2+}, (d) Mg^{2+}, (e) Al^{3+}, (f) Cr^{3+}, (g) Mn^{2+}, (h) Fe^{3+}, (i) Co^{2+}, (j) Ni^{2+}, (k) Cu^{2+}, (l) Zn^{2+}, (m) Cd^{2+}, (n) Hg^{2+} and (o) Pb^{2+}

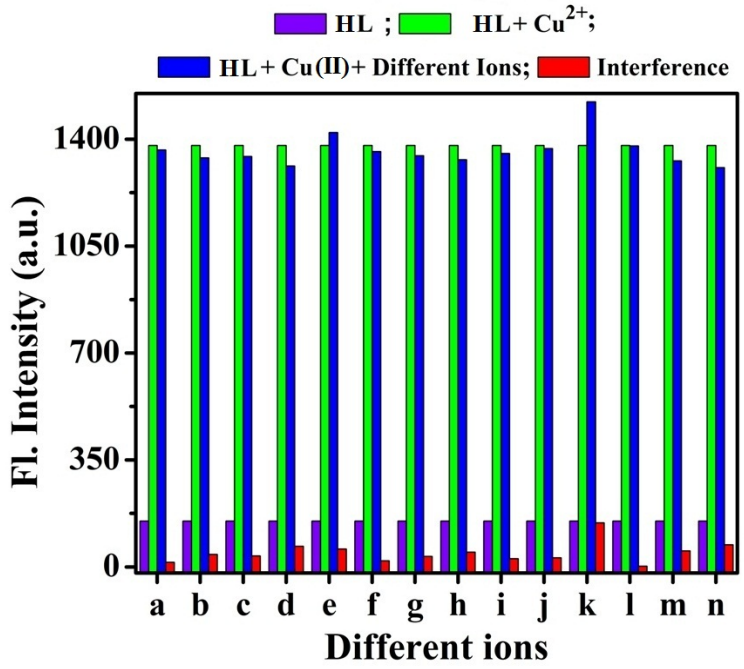

Fig. S19 Change of relative fluorescence intensity profile of **HL** in HEPES buffer (1 mM, pH 7.4; acetonitrile/water: 1/5, v/v) at 25 °C (λ_{ex} = 365 nm). (a) Na^{+}, (b) K^{+}, (c) Ca^{2+}, (d) Mg^{2+}, (e) Hg^{2+}, (f) Cr^{3+}, (g) Mn^{2+}, (h) Fe^{3+}, (i) Co^{2+}, (j) Ni^{2+}, (k) Al^{3+}, (l) Zn^{2+}, (m) Cd^{2+}, and (n) Pb^{2+}

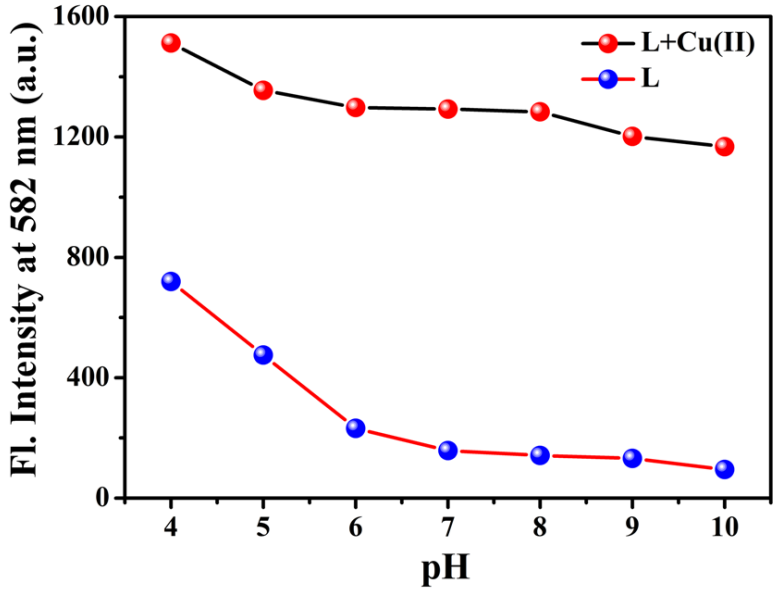

Fig. S20 pH Effect of **HL** in absence and in presence of Cu(II)

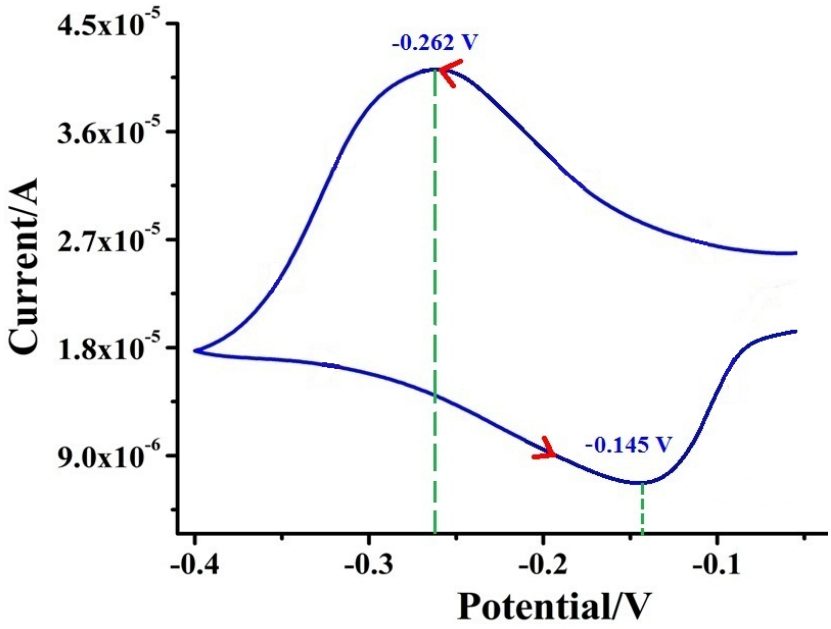

Fig. S21 Cyclic voltammogram (scan rate 100 mV/s) of (L-Cu) (**1**) complex in acetonitrile solution containing 0.1 M TBAP, using platinum working electrode

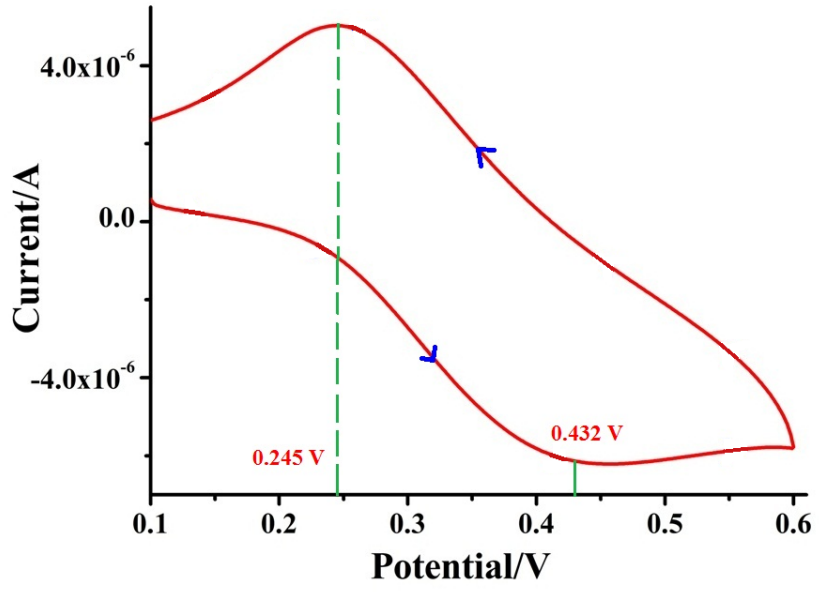

Fig. S22 Cyclic voltammogram (scan rate 100 mV/s) of (HL-Cu) (**2**) complex in acetonitrile solution containing 0.1 M TBAP, using platinum working electrode

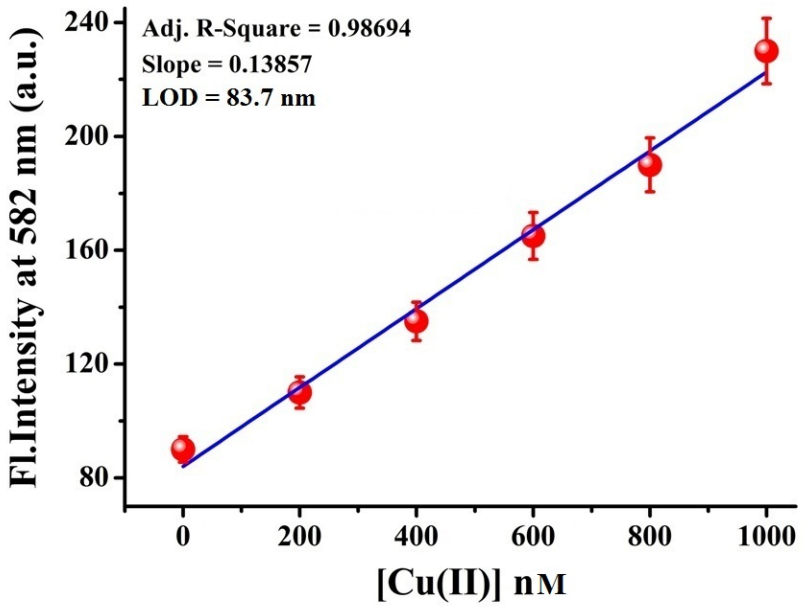

Fig. S23 Calibration curve for the nanomolar range, with error bars for calculating the LOD of Cu(II) by **HL** in HEPES buffer (1 mM, pH 7.4; acetonitrile/water: 1/5, v/v) at 25 °C

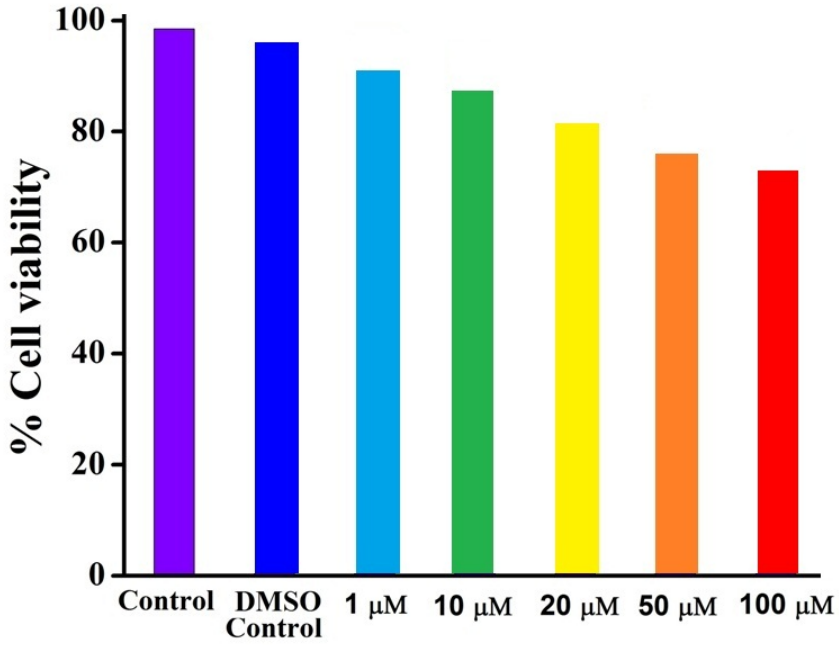

Fig. S24 Cytotoxic effect of **HL** (1, 10, 20, 50 and 100 μM) in HeLa cells incubated for 6 h

Table S1 Crystal data and details of refinements for **HL**

HL	
Empirical Formula	$C_{37}H_{37}N_5O_4$
Formula Weight	615.71
Crystal system	Monoclinic
Space group	P 21/n
a (Å)	8.9207(11)
b (Å)	23.567(3)
c (Å)	16.0637(19)
α	90°
β	104.889(9)
γ	90°
Volume (Å^3)	3263.7(7)
Temperature (K)	293(2)
Z	4
ρ_{calc} (g/cm^3)	1.253
μ (mm^{-1})	0.083
F(000)	1304
θ range (deg)	1.728-25.35
Reflections collected / unique	2687/5980
R indices (all data)	0.0761
Goodness-of-fit on F^2	1.017

Table S2A Selected bond distances (Å) for **HL**

HL	
O1 - N1	1.234(5)
O2 - N1	1.226(5)
O3 - C1	1.234(5)
O4 - C18	1.388(4)
O4 - C19	1.389(4)
N1 - C35	1.463(6)
N2 - C29	1.283(5)
N2 - N3	1.388(4)
N3 - C1	1.377(5)
N3 - C8	1.492(5)
N4 - C12	1.381(5)
N4 - C13	1.452(6)
N4 - C15	1.463(6)
N5 C21	1.395(5)
N5 C22	1.453(5)
N5 C24	1.541(8)

Table S2B Selected bond angles (°) for **HL**

HL	
C18 - O4 - C19	117.4(3)
O2 - N1 - O1	123.3(5)
O2 - N1 - C35	118.7(6)
O1 - N1 - C35	118.0(5)
C29 - N2 - N3	118.1(3)
C1 - N3 - N2	130.0(3)
C1 - N3 - C8	114.3(3)
N2 - N3 - C8	115.7(3)
C12 - N4 - C13	121.9(4)
C12 - N4 - C15	120.7(4)
C13 - N4 - C15	116.3(4)
C21 - N5 - C22	119.3(4)
C21 - N5 - C24	116.5(4)

Table S3 Life time detail of **HL** at 415 nm

	B_1	B_2	T_1(ns)	T_2(ns)	T_{av}(ns)	X^2	φ	K_r	K_{nr}
HL	18.35	81.65	1.19	5.41	4.64	1.079	0.34	0.073	0.142
HL + Cu(II) (1:0.5)	34.58	65.42	2.12	5.85	4.56	1.076	-	-	-
HL + Cu(II) (1:1)	31.0	69.0	1.95	5.39	4.32	1.030	0.11	0.025	0.206